Journal of Statistical Physics, Vol. 65, Nos. 3/4, 1991

Thermodynamics of a Model wih Interacting Annealed Bond Impurities on the Bethe Lattice

B. M. Mulder,[1] C. Krikos,[1] and C. Papatriantafillou[1]

Received October 10, 1990; final June 10, 1991

A magnetic model is considered consisting of annealed, mutually repelling ferromagnetic bond impurities in an antiferromagnetic host lattice. Using recurrence relation techniques, the grand-canonical version of this model is solved on the three-coordinated Bethe lattice. A generic phase diagram is obtained containing, apart from the usual ferro- and antiferromagnetic regimes, two distinct incommensurate phases as well as a period-four modulated phase. Evidence is obtained that in one of the two incommensurate phases impurity pairing occurs.

KEY WORDS: Ising model; Bond disorder; Bethe lattice.

1. INTRODUCTION

Recently several theories of high-temperature superconductivity of planar CuO_2 have been proposed on the basis of magnetic frustration effects.[1,2] In these theories oxygen impurities occupy sites between the copper atoms in certain planes of the host lattice. For low concentrations the electronic holes created by these impurities can be taken to be localized. Their effect is to change the initially antiferromagnetic exchange interactions between the host spins into ferromagnetic ones. The resultant frustration effects are then thought to cause a pairing interaction between the holes, thus leading to a possible mechanism for superconductivity. The aim of this paper is to study, on a classical level, the types of magnetic effects associated with such a model. To this end we will introduce an, albeit rather simplified, version of the above model containing, however, all the relevant ingredients, including a repulsive interaction between the impurities in order to model

[1] Institute for Materials Science, National Centre for Scientific Research "Demokritos," 153 10 Aghia Paraskevi Attikis, Greece.

0022-4715/91/1100-0423$06.50/0

the Coulomb repulsion due to their charges. This model will be introduced in Section 2. In order to obtain information about the behavior of our model we will need to resort to soe sort of approximation scheme. We choose to solve the model on a Bethe lattice using recurrence relation techniques that are especially suited to describing various forms of complex spatial ordering. This approach is discussed in Section 3. We go on to study the phase diagram of the system as well as the properties of the various relevant thermodynamic quantities. The results are discussed in Section 4. We close with a short discussion in Section 5.

2. DEFINITION OF THE MODEL

We start with a host system consisting of a lattice of Ising spins with a nearest neighbor antiferromagnetic coupling of strength J. Now consider introducing Ising spins as impurities on the bonds of the lattice that interact ferromagnetically with the host spins on the adjoining vertices through a coupling of strength $-J'$, but do not interact with other impurities, a model first studied by de'Bell.[3] Choosing $J' \geqslant J$ assigns the lowest energy to the state of a single bond where an impurity spin is present and all spins along the bond are aligned. Note that the presence and the state of an impurity are irrelevant when the vertex spins have opposite values. The state where none of the interactions along the bond are satisfied, i.e., with the vertex spins aligned oppositely to the impurity spin, will, given the condition on the relevant strengths, have a much larger energy than any of the other configurations. This leads us to propose the following simplification of the above: discard the highest energy bond configuration and disregard the higher multiplicity of the configurations with opposite values of the vertex spins. The result is model where only the presence of an impurity is relevant in that it changes the antiferromagnetic interaction between the vertex spins into a ferromagnetic one. This procedure is illustrated in Fig. 1. The energy of a bond configuration in the resulting model is given by

$$\mathscr{E}_{\text{bond}} = -J(\alpha\varepsilon_{ij} - 1)\sigma_i\sigma_j - J\alpha\varepsilon_{ij}, \qquad \alpha = J'/J \tag{1}$$

where ε_{ij} is an occupation variable taking the values 0 and 1 and the σ's are the Ising variables of the vertex spins. This effective spin–spin interaction is closely related to the one proposed by Kasai and Syozi[4] as the so-called excluded double-bond model. In order to take into account a mutual repulsion of the impurities, mimicking the effect of the Coulomb repulsion that is present when charged impurities are introduced into a real system, we add the following term to the Hamiltonian for each nearest-neighbor pair of bonds:

$$\mathscr{E}_{\text{imp-imp}} = \rho J\varepsilon_{ij}\varepsilon_{jk} \tag{2}$$

where $\rho \geqslant 0$ is a dimensionless parameter measuring the strength of the impurity repulsion relative to the spin–spin interaction. In order to control the average concentration of impurities present we will couple the system to a bath of impurities at a fixed chemical potential. We therefore add single-impurity energy terms to the Hamiltonian of the form

$$\mathscr{E}_{\text{bath}} = -J\mu\varepsilon_{ij} \tag{3}$$

which defines our dimensionless chemical potential μ. Before proceeding we will transform the impurity occupation variable ε to an Ising-type variable $\varepsilon = \frac{1}{2}(\tau + 1)$ which will simplify some of the later algebra. Omitting irrelevant constant terms, we obtain the bond configuration energy in the form

$$\mathscr{E}_{\text{bond}} = -J(A-1)\sigma_i\sigma_j - JA\tau_{ij}\sigma_i\sigma_j - JA\tau_{ij} \tag{4}$$

the impurity–impurity interaction by

$$\mathscr{E}_{\text{imp-imp}} = JR(\tau_{ij}\tau_{jk} + \tau_{ij} + \tau_{jk}) \tag{5}$$

and the interaction with the bath by

$$\mathscr{E}_{\text{bath}} = -JM\tau_{ij} \tag{6}$$

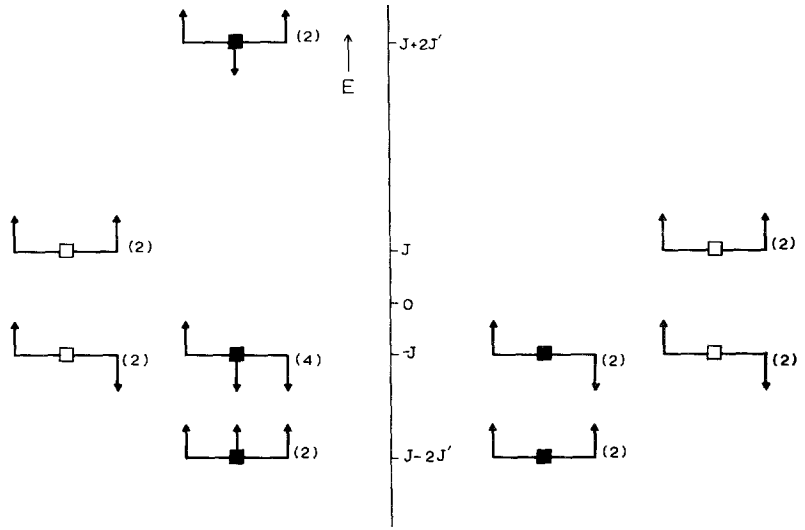

Fig. 1. Energy levels of bond configurations. Left: the original de'Bell model; right: our simplified version. A black square denotes occupancy by an impurity. The bracketed numbers are degeneracies.

where we have introduced the redefined parameters $A = \frac{1}{2}\alpha$, $R = \frac{1}{4}\rho$, and $M = \frac{1}{2}\mu$.

We would like to point out that the model proposed here is new in the sense that it combines both the influence of the bond impurities on the magnetic order of the host material as well as the interactions between the impurities themselves. Several models have been proposed[5,6] in relation to high-T_c superconductivity that consider the influence on the magnetic order due to the presence of oxygen impurities that change the sign of the host spin–spin interaction, but these do not take into account the repulsive interactions between the impurities. On the other hand, there are lattice gas Ising models proposed for the ordering of the oxygen atoms in the basal planes of superconductors (see the review by Szpilka *et al.*[7] and references therein), but these do not deal with the coupling to the magnetic degrees of freedom.

3. SOLUTION OF THE MODEL ON A BETHE LATTICE

There are at present only few techniques available for studying magnetic systems of the type described in the previous section. A fundamental difficulty is the fact that the interactions introduce an element of frustration in the system: The realization of the lowest bond-energy state comprised of fully decorated bonds with ferromagnetically aligned spins [see Eq. (1)] is incompatible with the repulsive interimpurity interaction (2) that disfavors impurity clustering. The result is that these systems can develop spatially modulated phases of varying degrees of complexity. A model of this type that has been extensively studied is the ANNNI model.[8] In this case even the application of standard mean-field theory on cubic lattices becomes an involved problem.[9] An alternative approach toward this type of model is to study them on the Bethe lattice.[10–12] A major advantage of this approach is that it yields recursive equations for the local thermodynamic quantities which allow, in principle, a complete analysis of the "spatial" structures that appear. Of course by considering only the simple branching topology of the Bethe lattice one misses out on geometry-related effects relevant to real lattices. As such the results of this approach should be considered as indicative for the behavior on real lattices.

We will consider the model as defined in Section 2 on a Bethe lattice with coordination number $z = 3$. Given the fact that on a Bethe lattice, in contrast to a real lattice, any bond impinging on a single site has to be considered nearest neighbor to any of the other bonds connected to the same site, the impurity–impurity interaction as defined in (2) becomes effectively isotropic. We therefore assume that the dependence of the

overall features of the system on the coordination number is slight. This justifies our choice of the lowest relevant coordination number, which considerably simplifies the analytical treatment necessary.

Our treatment of the problem is a generalization of an idea originally due to Morita.[13] Similar and equivalent techniques are described in refs. 14 and 15. Consider an isometric Cayley tree of radius $\mathscr{R}$, which is the distance from he central site to any site on its surface, with the distance between two sites being defined as the minimum number of bonds one needs to traverse to reach the one site starting from the other. We moreover assume that homogeneous boundary conditions are enforced at the surface of the tree. One now defines a *branch* $\mathscr{B}_{i;j}$ of the tree by selecting a site i and one of the bonds $\langle ij \rangle$ connected to it and considering the set of all sites connected to i by shortest-distance paths that pass through the bond $\langle ij \rangle$ (see Fig. 2). Fixing the value of the spin σ_i on the selected site and the value of the impurity variable τ_{ij} on the selected bond—we will refer to this combination of spin site plus impurity site as the *stem* of the branch—one then defines the branch partition sum $\mathscr{Q}_{i;j}(\sigma_i, \tau_{ij})$ obtained by summing the Boltzmann weight of the selected branch over all degrees of freedom in the branch apart from the two fixed at its stem, i.e.,

$$\mathscr{Q}_{i;j}(\sigma_i, \tau_{ij}) = \sum_{\substack{\{\sigma_k, \tau_{kl}, \text{ in } \mathscr{B}_{i;j}\} \\ \sigma_i, \tau_{ij} \text{ fixed}}} \prod_{\langle nm \rangle} \exp[-\beta \mathscr{E}_{\text{bond}}(\sigma_n, \sigma_m, \tau_{nm})] \times \prod_{\langle nm, ml \rangle} \exp[-\beta \mathscr{E}_{\text{imp-imp}}(\tau_{nm}, \tau_{ml})] \prod_{\langle nm \rangle} \exp[-\beta \mathscr{E}_{\text{bath}}(\tau_{nm})] \tag{7}$$

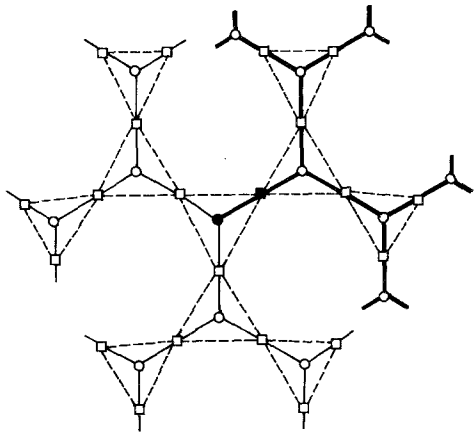

Fig. 2. The three-coordinated Bethe lattice. The solid lines are the bonds connecting the spins, which are located on the circles. The sites which can be occupied by impurities are shown as squares on the bonds. The dashed lines represent the interimpurity interaction. The thicker bonds define a branch of the tree which has the black spin and impurity site as its stem.

This summation can be recursively evaluated, since the summand splits into independent factors along the bonds leading out from the second site j, the summations over these individual factors being identical in structure to (7). This procedure is symbolically depicted in Fig. 3. Explicitly this recursion is given by

$$\begin{aligned}\mathcal{Q}_{i;j}(\sigma,\tau) &= \exp[K(A+M-2R)\tau] \\ &\times \sum_{\sigma',\tau',\tau''} \exp\{K[(A-1)\sigma\sigma' + A\tau\sigma\sigma' - R(\tau\tau' + \tau\tau'' + \tau'\tau'' + 2\tau' + 2\tau'')]\} \\ &\times \mathcal{Q}_{j;j'}(\sigma',\tau')\,\mathcal{Q}_{j;j''}(\sigma',\tau'') \end{aligned} \tag{8}$$

where we have introduced the dimensionless inverse temperature $K=\beta J$. It is convenient introduce the following parametrization for the $\mathcal{Q}$'s:

$$\mathcal{Q}(\sigma,\tau) = q\{1 + x\sigma + y\tau + z\sigma\tau\} \tag{9}$$

where, in order to ensure positivity, we have $q \geqslant 0$ and (x, y, z) considered as a point in three-space must lie in the tetrahedron with vertices (1, 1, 1), (1, −1, −1), (−1, 1, −1), and (−1, −1, 1). Insertion into (8) leads to

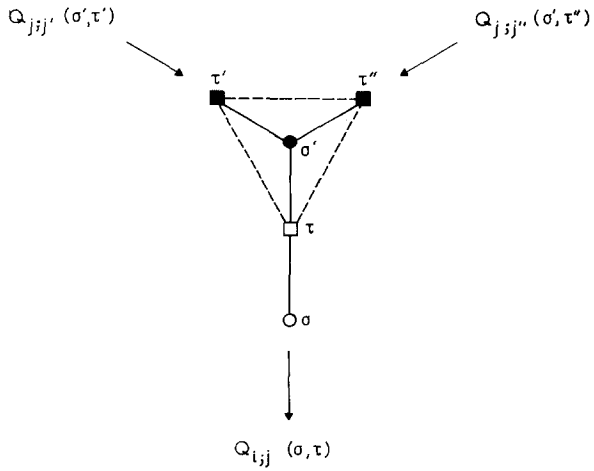

Fig. 3. Symbolic representation of the recursion relation. The new branch partition sum is obtained by forming the product of all Boltzmann weights associated with the diagram and the two incoming branch sums and summing over the degrees of freedom in the filled-in circle and squares.

a closed set of coupled recursion equations involving *only* the variables (x, y, z):

$$\begin{aligned} x &= X((x', y', z'), (x'', y'', z'')) \\ y &= Y((x', y', z'), (x'', y'', z'')) \\ z &= Z(x', y', z'), (x'', y'', z'')) \end{aligned} \tag{10}$$

where, for reasons of notational economy, we have dropped the site labels identifying the stems of the branches involved. We refer the reader to Appendix A for the explicit expressions of the functions X, Y, and Z, which are ratios of second-degree polynomials of their variables. To make contact with local thermodynamic variables we note that the configuration probability of an elementary *triangle* cluster, consisting of a given spin and the three impurity sites on the bonds impinging on this spin, can be expressed in terms of the branch partition functions of the three branches that have the selected spin as their root. Explicitly, we have

$$\begin{aligned} &P_{i,j,j',j''}(\sigma, \tau, \tau', \tau'') \\ &\quad = \frac{1}{N} \exp[-KR(\tau\tau' + \tau\tau'' + \tau'\tau'' + 2\tau + 2\tau' + 2\tau'')] \\ &\qquad \times \mathcal{Q}_{i;j}(\sigma, \tau)\, \mathcal{Q}_{i;j'}(\sigma, \tau')\, \mathcal{Q}_{i;j''}(\sigma, \tau'') \end{aligned} \tag{11}$$

where N is chosen to normalize the probability. The product structure with respect to the $\mathcal{Q}$'s, which reflects the branching nature of the lattice, ensures that we can absorb the multiplicative factors q, which appear in the parametrization (9) and are left undetermined by the recursion equations (10), into the normalization constant N, enabling the probability to be expressed solely in terms of the variables (x, y, z). We refer the reader to Appendix B for the relevant expressions. In order to obtain the so-called *interior* properties of the system, i.e., the properties sufficiently far away from the surface so that transient effects due to the boundary conditions have disappeared, we adopt the following procedure. First we iterate (10) starting from the boundary and moving deeper into the the tree. This iteration can be labeled by an index denoting the distance of the root spin to the surface. Since we assume homogeneous boundary conditions, we do not need to differentiate between the contributions of the two ingoing branches, i.e., we have an iteration of the form

$$\begin{aligned} x_l &= \xi(x_{l-1}, y_{l-1}, z_{l-1}) \\ y_l &= \eta(x_{l-1}, y_{l-1}, z_{l-1}) \\ z_l &= \zeta(x_{l-1}, y_{l-1}, z_{l-1}) \end{aligned} \tag{12}$$

where $l = 1, 2, \ldots$ and $\xi(x, y, z) = X((x, y, z), (x, y, z))$, etc. [see (A4)]. This process is repeated K times, with K chosen such that transient effects have died out and all iterations fall on an attractor of the recurrence equations. We then continue for another L steps, storing the results $(x_{K+k}, y_{K+k}, z_{K+k})_{k=1,2,\ldots,L}$. The site reached after these L steps is then arbitrarily chosen to be the central site of the tree. Applying Eqs. (10), we can then calculate the $\mathcal{Q}$'s of the branches that have their stems pointing in the reverse direction, i.e., toward the surface of the tree. Denoting by $(\tilde{x}, \tilde{y}, \tilde{z})$ the parametrization of these *out*going contributions, we have the following recursion:

$$\begin{aligned} \tilde{x}_l &= X((x_l, y_l, z_l), (\tilde{x}_{l+1}, \tilde{y}_{l+1}, \tilde{z}_{l+1})) \\ \tilde{y}_l &= Y((x_l, y_l, z_l), (\tilde{x}_{l+1}, \tilde{y}_{l+1}, \tilde{z}_{l+1})) \\ \tilde{z}_l &= Z((x_l, y_l, z_l), (\tilde{x}_{l+1}, \tilde{y}_{l+1}, \tilde{z}_{l+1})) \\ l &= K+L, K+L-1, \ldots, K+1 \end{aligned} \tag{13}$$

with boundary conditions

$$\tilde{x}_{K+L+1} = x_{K+L}, \qquad \tilde{y}_{K+L+1} = y_{K+L}, \qquad \tilde{z}_{K+L+1} = z_{K+L} \tag{14}$$

where l again labels the level of the tree counted from the surface and the (x_l, y_l, z_l) are the previously stored parameters of the *in*going contributions. Simultaneously at each step we can calculate several thermodynamic quantities of interest, such as the magnetization, the impurity concentration, and various impurity-pair configuration probabilities, using our result for the elementary triangle probability (11).

4. RESULTS

In this section we discuss some of the results we obtained on the system described in Section 2, using the methods outlined in Section 3. Unless stated otherwise, the results pertain to the case where the parameter governing the ratio of the ferro- to antiferromagnetic coupling has the value $\alpha = 2.0$ and the parameter defining the strength of the impurity–impurity repulsion has the value $\rho = 1.5$. Note that this value of the parameter α corresponds to the case where the ferromagnetic coupling induced by the presence of an impurity is equal in *magnitude* to the strength of the host antiferromagnetic coupling. In the absence of the repulsive interaction between the impurities ($\rho = 0$) this system would therefore possess a symmetry with respect to the interchange of the average concentration of impurities with the average concentration of nonoccupied bonds. Any observed asymmetries between the low-impurity-concentration

regime and the high-impurity-concentration regie are therefore due to the impurity–impurity repulsion.

In Fig. 4 we present the chemical potential versus temperature ($T = 1/K$) phase diagram of the system for those temperatures which were accessible using our method. We observed that there is a chemical-potential-dependent temperature below which the recurrence relations (12) show numerical instabilities due to the fact that both the numerator and the denominator of the algebraic functions defining the recurrence become small. This effect is probably the sympton of a nonanalytic dependence of the average impurity concentration as a function of the chemical potential at zero temperature. A full analysis of this behavior is possible only for the simpler case with noninteracting impurities ($\rho = 0$),[16] so that in this work we are forced to accept this limitation on the determination of the low-temperature region of the phase diagram.

Apart from the expected antiferromagnetic phase (AF) for small μ (corresponding to a low impurity concentration) and ferromagnetic (F) phase for high μ (high impurity concentration) we find an "island" in the phase diagram consisting of two incommensurate phases, which we denote by I and I′, separated by a modulated phase M. We have also performed a linear stability analysis of the recursion equations in order to obtain the location of the paramagnetic phase boundaries directly. This shows that the apparent kink in the meeting point of the P–I and P–I′ lines in the P–M–I–I′ multicritical point is an artifact of the scale: the two lines

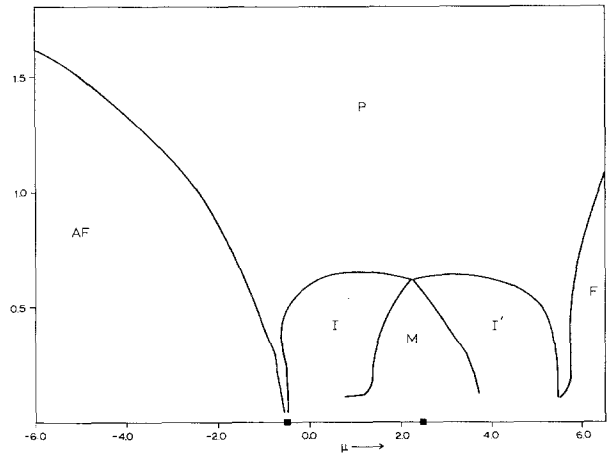

Fig. 4. The chemical potential versus temperature phase diagram for our model with $\alpha = 2$ and $\rho = 1.5$. P: paramagnetic phase. AF: antiferromagnetic phase. I, I′: Incommensurate phases. M: period-four modulated phase. The black squares denote the predicted location of the zero-temperature transitions that destabilize the AF and F phases, respectively.

smoothly merge together with zero slope with respect to μ at the multicritical point. Unfortunately, the linear stability analysis is plagued by the same numerical problems as the recursion relations themselves, so it does not help in obtaining more information about the phase boundaries in the low-temperature "inaccesible" region.

The nature of the various phases can be identified by studying phase plots of the variables obtained in the ingoing iteration. In Fig. 5 we present some of these plots for the "magnetic" variable x_l, clearly showing the nature of the attractor in each case. The modulated phase has a magnetic signature of type $(+ + - -)$, while the incommensurate phases, locally having this same pattern, show nonperiodic behavior due to random isolated deviations from this pattern.

As far as we could determine, the "island" in the phase diagram is always separated from the flanking ferro- and antiferromagnetic phases by a narrow paramagnetic (P) region. We conjecture that this paramagnetic gap remains finite at any finite temperature, vanishing exactly at $T=0$. In fact we speculate that the location of the points on the zero-temperature axis, where, at constant chemical potential, the antiferromagnetic phase with zero impurity concentration and the ferromagnetic phase with unit impurity concentration transform into a more complex ground-state phase, can be determined by the following argument.

(i) Consider a perfect antiferromagnetic ground state without impurities. Flip a single spin, creating three ferromagnetically ordered bonds, and add three impurities to satisfy the spin–spin interaction along these bonds. If the grand canonical weight of the new configuration is equal to the old one, the AF ground state becomes instable to *isolated* disturbances of the above type. Using the definitions of the weights (4)–(6), one finds that the above criterion determines the critical chemical potential

$$\mu_{\mathrm{AF}}^{*}=2-2\alpha+\rho \tag{15}$$

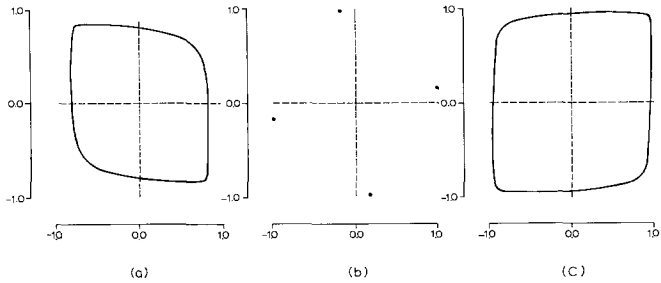

Fig. 5. Phase plots of the recursion equations for the "magnetic" variable x. Horizontal axis: x_l. Vertical axis: x_{l+1}. (a) The incommensurate phase I, (b) the modulated phase M, (c) the incommensurate phase I′.

(ii) Completely analogous to the above, we consider a fully decorated, perfectly ordered ferromagnetic state and flip a single spin while removing three impurities. Again equalizing the respective grand canonical weights, we obtain a second critical chemical potential

$$\mu^*_{\mathrm{AF}} = 2 - 2\alpha + 3\rho \tag{16}$$

In the case $\rho = 0$ the two critical values coincide and the result agrees with the exact analysis of ref. 16. Looking at the phase diagram in Fig. 4, where we have marked these critical values on the $T = 0$ axis, one sees that μ^*_{AF} correlates quite well to the data obtained. The verdict is still out on μ^*_{F}, there being only a slight indication that the P–F phase boundary bends inward toward lower values of μ at the lowest temperatures we were able to study.

Since, from a physical point of view, we are more interested in the behavior of the system at fixed *average* impurity concentration, we have studied the dependence of this quantity on the chemical potential at constant temperature. We define the average concentration as determined by our calculations as

$$\bar{n} = \frac{1}{L} \sum_{i=1}^{L} n_{K+i} \tag{17}$$

where n_l is the impurity concentration on level l from the surface as determined from (B9), and K and L were defined in Section 3. The length of our "measurement" interval was typically chosen to be $L = 1000$, large enough to obtain a good averaging in the case of the incommensurate phases I and I′ and trivially correct for the remaining phases that are periodic with period lengths one (P and F), two (AF), and four (M), respectively. In Fig. 6 we show a typical low-temperature graph ($T = 0.25$) of the average impurity concentration. We observe that the $\bar{n}$ increases strictly monotically with increasing μ, with the exception of the modulated phase M, wherein it remains constant and equal to $\bar{n} = 0.5$ independently of the temperature. Figure 7 presents the relevant part of the graph at a much higher resolution for the case $T = 0.5$, clearly displaying this plateau of constant average concentration. Thermodynamically speaking, the presence of this flat part in the chemical potential versus average concentration curve means that at *constant* impurity concentration one *cannot* observe the modulated phase M, which apparently is an artifact of the coupling with the impurity bath. Instead one would observe, on increasing the impurity concentration of the system, a direct transition between the two incommensurate phases I and I′. This behavior of the system is

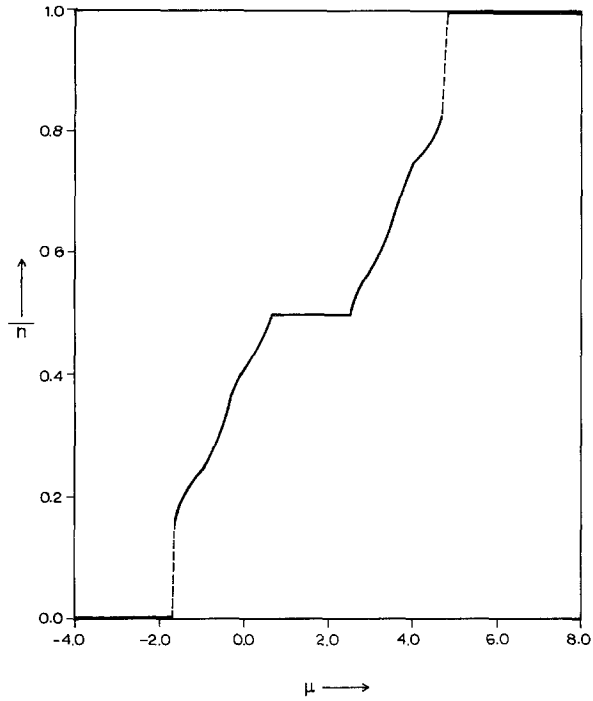

Fig. 6. The average impurity density $\bar{n}$ as a function of the chemical potential for $T = 0.25$.

another interesting example of the nonequivalence of ensembles that seems to occur in the presence of competing annealed interactions.[16] A final close-up at $T = 0.25$ of the μ–$\bar{n}$ isotherm in the region around the AF–P–I transition in Fig. 8 shows that the average concentration shows a jump discontinuity at the antiferromagnetic to paramagnetic transition (the same happens at the high-concentration paramagnetic to ferromagnetic transition). This would indicate that at the fixed average impurity concentration there might exist intermediate concentration phases unobservable in this grand-canonical approach. To answer these questions one would need to study an appropriate thermodynamic potential, which is not straightforward to construct from our essentially local analysis of the lattice properties.

As stated in the introduction, we are interested in examining the possibility of impurity pairing. We therefore take a closer look at the incommensurate phase I. We restrict ourselves to this case, since we have established that in the other incommensurate phase I′ the average impurity density $\bar{n}$ is larger than 1/2, while on our lattice a close-packed configuration of isolated impurity pairs would have an average density $\bar{n}_{cp} = 1/2$. We thus

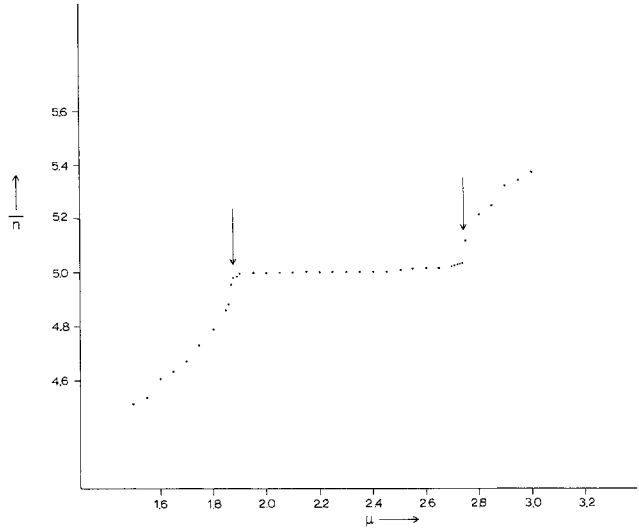

Fig. 7. Closeup of the plateau of the average impurity density at $T=0.5$ in the modulated phase M. Note the expanded scale of the density (units are 10^{-1}). The arrows denote the location of the phase transition as determined from the recursion equations.

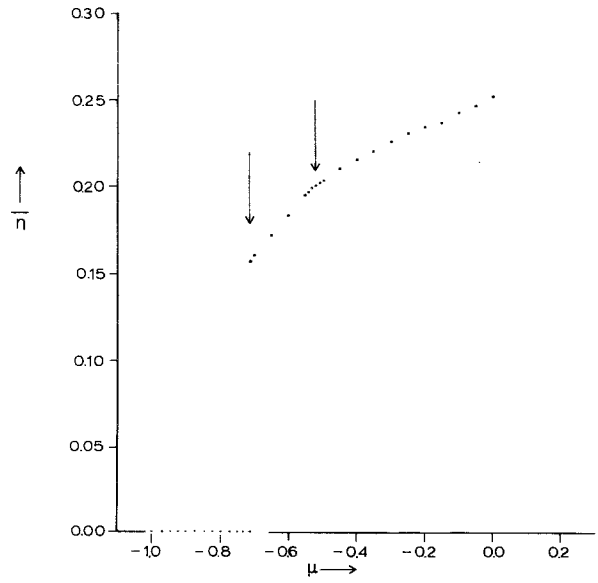

Fig. 8. The jump discontinuity of the average impurity density at the AF to P boundary ($T=0.25$). The arrows locate the AF–P and the P–I transitions, respectively.

expect isolated impurity pairs, if any, to appear in I. From the elementary triangle probability (11) we can compute the probabilities of several impurity configurations on this triangle. Averaging these results over our measurement interval—the M shells of the tree closest to the center—we can obtain some partial information on the pairing behavior.

Note that each elementary triangle has a unique orientation with respect to the tree, two of its impurity vertices "pointing" toward the surface and one toward the center. This is of interest since, as we shall see, in the incommensurate phases the threefold symmetry of the various configurations on the triangle is broken. Of course the geometry of our system consisting of an isometric tree with boundary constrains this symmetry breaking to have a twofold axis along the direction orthogonal to the successive shells of the tree, but this entails no loss of generality, since on the infinite tree without boundaries we expect a phase with broken occupation symmetry to be threefold degenerate. Our method of solving for the interior properties of the tree simply selects one of these three possibilities. Likewise we do not expect the assumption of the homogeneity of the boundary conditions to play a role in the determination of the phase behavior, since at every level of the tree the recursion relations preform an averaging over the contributions of the different incoming branches, a process which washes out any inhomogeneities of finite extent within a few iterations.

For ease of reference we will call the impurity pair consisting of the two "surface" sites *tangential* and any other pair *radial.* In Fig. 9 we show the average probabilities of a few relevant impurity configurations as a

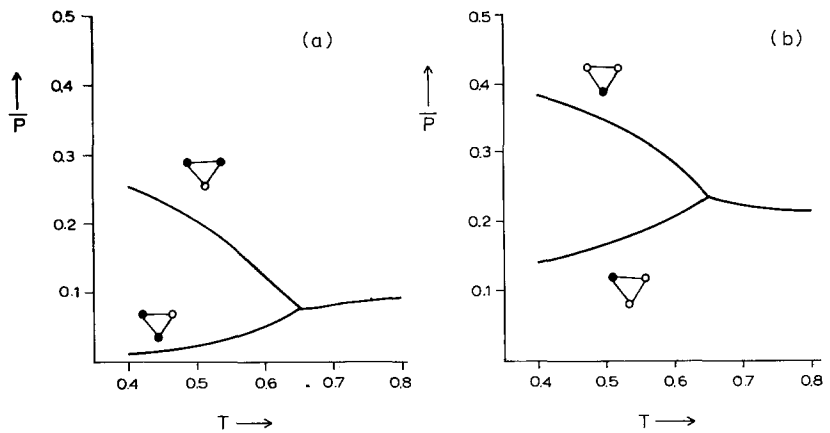

Fig. 9. The average probabilities $\bar{P}$ for various impurity configurations on the elementary triangle on a constant-chemical-potential ($\mu = 1$) cut in the phase diagram that crosses the paramagnetic to incommensurate I phase boundary.

function of temperature along a line of constant chemical potential $\mu = 1$, chosen to intersect the phase I somewhere in the middle. We do not show the average probability of *full* occupation of the triangle, since this turned out to be negligible in the regime considered. The most marked phenomenon we observe in the I phase is the rapid increase of tangential pairs coupled to a decrease of radial pairs. The low probability of radial pairs also implies the low probability of wedge-shaped triplets obtained by combining a radial and a tangential pair on two successive triangles. We thus infer that the probability of the tangential pairs is a good measure for the probability of isolated pairs. The picture of the I phase that emerges is thus one of a mixture of isolated tangential pairs and singlets. On crossing the paramagnetic to incommensurate boundary, we have a simultaneous increase of the number of tangential pairs coupled to a suppression of the wedge triplets. Ideally one should consider the probability of a much larger cluster in order to obtain the isolated pair probabilities directly. We nevertheless believe that the information obtained through our method contains strong indications of a pairing phenomenon occurring in the incommensurate I phase.

Finally we turn to the question of the dependence of the observed phases on the two parameters of our model: α and ρ. We have observed that for all values of $\alpha > 1$ and $\rho > 0$ we have considered, the topology of the phase diagram in the accessible regime of temperatures remains the same. Of course the locations of the phase boundaries depend on the actual

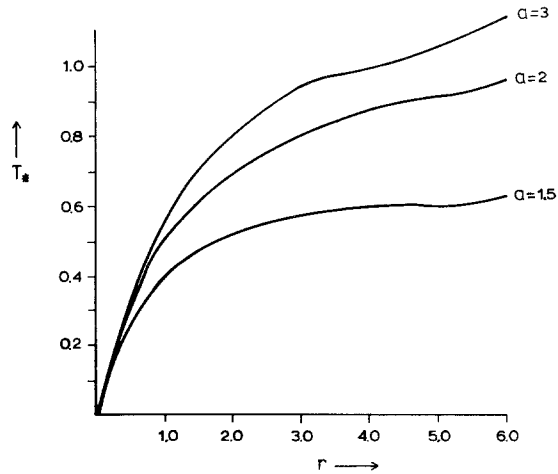

Fig. 10. The temperature T^* of the P–I–M–I′ multicritical point in the phase diagram as a function of the parameter ρ measuring the strength of the interimpurity repulsion for various values of the parameter α measuring the relative strength of the undecorated antiferromagnetic interaction with respect to the decorated ferromagnetic interaction.

values of the parameters. As a crude measure of the influence of the parameters, we plot in Fig. 10 the value of the temperature associated with the P–I–M–I′ multicritical point in the phase diagram (see Fig. 4) as a function of ρ for various values of α. There is no evidence for a critical lower bound on ρ below which the new spatially varying phases I, M, and I′ do not appear at sufficiently low temperature.

5. CONCLUSIONS

In this paper we have studied what is arguably the simplest model describing the effects of competing magnetic ordering due to interacting impurities. The interplay between the competing magnetic interactions which energetically favor the presence of impurities and the repulsive impurity–impurity interaction which disfavors their clustering introduces a measure of frustration into the system, which manifests itself in the appearance of modulated and incommensurate phases. Although the term frustration has come to be associated solely with the plaquette frustration typical of spin glasses,[17] we feel that this term is appropriate for every model in which there is no configuration of the microscopic variables that simultaneously satisfies, i.e., minimizes, all the interactions in the system individually, the plaquette frustrated systems being a special case of this type of model. This same feature is also present in our model, although caused by two different mechanisms, one indirect and one direct, the relative importance of which depends on the concentration of impurities. The indirect mechanism is due to the fixed spins on the boundary of the tree that preclude global rearrangements of the spins to accommodate the change of sign of even a single bond in the system. It is this influence of the boundary that causes the Bethe lattice, although not possessing closed loops, to admit even a spin-glass phase in the quenched $\pm J$ model, as was discussed by Chayes *et al.*[18] The direct mechanism arises from the fact that for all impurity concentrations $\geqslant 1/3$ there are by necessity dissatisfied impurity–impurity bonds. That these mechanisms lead to incommensurate phases in the range of concentrations roughly between $\bar{n}=1/3$ and $\bar{n}=2/3$ is probably due to the fact that in this regime the magnetic ordering that effectively homogenizes the system cannot operate because neither the antiferro- nor ferromagnetic bonds dominate, so that the configuration of the impurities becomes the prime determinant of the properties of the phases. Since for a generic value of the average concentration a regular arrangement of impurities would presummably require a large period to be realized, the intermediate solution of an incommensurate phase that locally resembles a modulated phase with a period of a few lattice constants but is globally adapted to yield the specified overall

concentration seems reasonable if only from an entropic point of view. The overall structure of the phase diagram, however, remains simple as compared to that found in the more "hard-wired" models frustrated in the sense outlined above, such as the ANNNI model, which have fixed bonds that enforce the nonexistence of lowest energy state that satisfies all bonds simultaneously. This difference is evidently due to the fact that in our case the impurities, which are the carriers of the frustration, are allowed to equilibrate with the host system, resulting in a marked softening of all effects.

The most intriguing aspect of our model is the evidence for the appearance of impurity pairing as found in the incommensurate I phase. In our formulation the origin for this effect lies in the presence of the repulsive interimpurity interaction. This is of course not the only mechanism one could propose to obtain such an effect. Pareskevaidis and Papatriantafillou[19] have recently studied the influence of magnetic fields on the noninteracting impurity version of the model presented here. They found that at low temperatures the magnetic fields also induce impurity clustering. Nevertheless, it is clear that in the real doped systems, such as those considered in high-T_c research, the Coulomb repulsion between the charged impurities should play a nonnegligible role. Anyway, in order to understand the type of magnetic phase diagram of superconductors presented in ref. 2, a new mechanism seems indispensable. Models based solely on the presence of annealed ferromagnetic bond impurities[5,6] are able to describe the disappearance of the antiferromagnetic phase with increasing doping, but this is just one aspect of the phase diagram. A spin-glass phase at higher impurity concentrations could be obtained by introducing a pinning mechanism that effectively quenches the impurities, but this is not a good candidate for the superconducting phase. We hope that our model, which of course does not propose a solution for the problem of high-T_c superconductivity, nevertheless, by demonstrating the possibility of new types of a phases in systems of interacting magnetic bond impurities, will stimulate possible new point of view in this matter.

An important question is, of course, whether any of the behavior which our model displays on the Bethe lattice will survive on, say, the two-dimensional square lattice, being the geometry most relevant to the description of basal-plane CuO superconductors. While this is a difficult question to answer in general and, given the state of the art as far as theory is concerned, will probably require large-scale simulation, a few remarks can be made. First of all the model without repulsion between the impurities can be exactly solved on the square lattice using the Syozi bond decoration transformation, which maps it onto an ordinary Ising model,[4] and its phase diagram does not differ from that on the Bethe lattice.[16] Second, the

mechanisms which we identified as causing the nontrivial behavior in the interacting case—the opposing tendencies of clustering due to the magnetic interactions and the counteracting interimpurity repulsions—remain operative on the regular lattice, although one will have to take into account geometric features of the lattice, i.e., a more realistic form of the interimpurity repulsions, as proposed, for instance, in ref. 7. An important ingredient seems to be the possibility of realizing a modulated phase of isolated pairs analogous to the M phase found on the Bethe lattice, since it is the short-range order of this phase that dominates the incommensurate phases I and I′. Candidates for such phases are easily constructed, and should be feasible low-energy states for suitable choices of the interaction parameters.

Finally we would like to remark that the analysis of our model as presented in this paper is not yet exhaustive. The low-temperature behavior certainly needs more study. In fact, we have seen evidence for more complex behavior, e.g., larger cycle modulated phases and even true chaotic phases. These states, however, occur in the region of the phase diagram where we encountered the numerical difficulties mentioned in Section 4, so we have not been able to study them systematically. Here one should either develop a different approach to the problem that bypasses the difficulties mentioned above, or turn to an even more drastic approximation like the mean-field limit obtained by studying the model on an infinitely coordinated tree with infinitely weak couplings,[12] which will reduce the number of independent variables from three to two.

APPENDIX A. THE RECURSION EQUATIONS

In this appendix we give the explicit formulas for the recurrence relations (10). They are obtained by inserting the parametrization (9) of the branch partition functions $\mathcal{Q}$ and expanding most of the exponentials using the identity $\exp(\sigma C) = \cosh(C) + \sigma \sinh(C)$ for $|\sigma| = 1$. First we introduce the useful notation $t_\lambda = \tanh(\lambda K)$ for a frequently occurring expression. Next we use the symmetric polynomials

$$\begin{aligned} p_0 &= 1 + x'x'' \\ p_1 &= x' + x'' \\ p_2 &= y' + y'' + x'z'' + x''z' \\ p_3 &= x'y'' + x''y' + z' + z'' \\ p_4 &= y'y'' + z'z'' \\ p_5 &= y'z'' + y''z' \end{aligned} \tag{A1}$$

and the parameters

$$\begin{aligned} a_0 &= 1 - t_R t_{3R}^2 & b_0 &= 1 - t_R^3 \\ a_1 &= t_{2A-1}(1 - t_R t_{3R}^2) & b_1 &= t_1(1 - t_R^3) \\ a_2 &= t_R t_{3R} - t_{3R} & b_2 &= t_R^2 - t_R \\ a_3 &= t_{2A-1}(t_R t_{3R} - t_{3R}) & b_3 &= t_1(t_R^2 - t_R) \\ a_4 &= t_{3R}^2 - t_R & b_4 &= t_R^2 - t_R \\ a_5 &= t_{2A-1}(t_{3R}^2 - t_R) & b_5 &= t_1(t_R^2 - t_R) \end{aligned} \tag{A2}$$

from which we form the terms

$$\begin{aligned} q_{+,+} &= a_0 p_0 + a_1 p_1 + a_2 p_2 + a_3 p_3 + a_4 p_4 + a_5 p_5 \\ q_{+,-} &= b_0 p_0 - b_1 p_1 + b_2 p_2 - b_3 p_3 + b_4 p_4 - b_5 p_5 \\ q_{-,+} &= a_0 p_0 - a_1 p_1 + a_2 p_2 - a_3 p_3 + a_4 p_4 - a_5 p_5 \\ q_{-,-} &= b_0 p_0 + b_1 p_1 + b_2 p_2 + b_3 p_3 + b_4 p_4 + b_5 p_5 \end{aligned} \tag{A3}$$

Finally, using the abbreviation $E = \exp[A + M - 2R)K]$, we get

$$\begin{aligned} X((x', y', z'), (x'', y'', z'')) &= \frac{E(q_{+,+} - q_{-,+}) + E^{-1}(q_{+,-} - q_{-,-})}{E(q_{+,+} + q_{-,+}) + E^{-1}(q_{+,-} + q_{-,-})} \\ Y((x', y', z'), (x'', y'', z'')) &= \frac{E(q_{+,+} + q_{-,+}) - E^{-1}(q_{+,-} + q_{-,-})}{E(q_{+,+} + q_{-,+}) + E^{-1}(q_{+,-} + q_{-,-})} \\ Z((x', y', z'), (x'', y'', z'')) &= \frac{E(q_{+,+} - q_{-,+}) - E^{-1}(q_{+,-} - q_{-,-})}{E(q_{+,+} + q_{-,+}) + E^{-1}(q_{+,-} + q_{-,-})} \end{aligned} \tag{A4}$$

APPENDIX B. THE TRIANGLE CLUSTER PROBABILITY

The algebra needed for obtaining the probability of the states on the elementary triangle is simplified by introducing the following set of basis functions of the triangle cluster configuration space:

$$\Delta_{i;jkl} = \sigma^i \tau_1^j \tau_2^k \tau_3^1, \qquad i, j, k, l = 0, 1 \tag{B1}$$

which allows us to expand

$$P(\sigma, \tau_1, \tau_2, \tau_3) = \frac{1}{16 c_{0;000}} \sum_{i,j,k,l=0}^{1} c_{i;jkl} \Delta_{i;jkl} \tag{B2}$$

Note that the product of two such basis functions is given by the simple rule

$$\Delta_{i;jkl}\,\Delta_{i';j'k'l'} = \Delta_{i\neq i';\,j\neq j'\,k\neq k'\,l\neq l'} \tag{B3}$$

where the $\#$ denotes the logical exclusive disjunction (XOR). The triple product of $\mathcal{Q}$'s appearing in (11) is expanded as

$$\mathcal{Q}_1(\sigma,\tau_1)\,\mathcal{Q}_2(\sigma,\tau_2)\,\mathcal{Q}_3(\sigma,\tau_3) = q_1 q_2 q_3 \sum_{i,j,k,l=0}^{1} p_{i;jkl}\,\Delta_{i;jkl} \tag{B4}$$

where the coefficients $p_{i;jkl}$ are the following polynomials in the variables $(x_n, y_n, z_n)_{n=1,2,3}$:

$$\begin{aligned}
p_{0;000} &= 1 + x_1x_2 + x_1x_3 + x_2x_3\\
p_{1;000} &= x_1 + x_2 + x_3 + x_1x_2x_3\\
p_{0;100} &= y_1(1 + x_2x_3) + (x_2 + x_3)z_1\\
p_{1;100} &= (x_2 + x_3)\,y_1 + (1 + x_2x_3)z_1\\
p_{0;110} &= y_1\,y_2 + z_1z_2 + x_3(y_1z_2 + y_2z_1)\\
p_{1;110} &= y_1z_2 + y_2z_1 + x_3(y_1\,y_2 + z_1z_2)\\
p_{0;111} &= y_1\,y_2\,y_3 + y_1z_2z_3 + y_3z_1z_2 + y_2z_3z_1\\
p_{1;111} &= y_1\,y_2z_3 + y_3\,y_1z_2 + y_2\,y_3z_1 + z_1z_2z_3
\end{aligned} \tag{B5}$$

with the remaining terms obtained by cyclic permutations of the labels (1, 2, 3). In the same manner the exponential factor in (11) describing the intratriangle impurity–impurity interactions can be expanded as

$$\begin{aligned}
&\exp[-KR(\tau_1\tau_2 + \tau_1\tau_3 + \tau_2\tau_3 + 2\tau_1 + 2\tau_2 + 2\tau_3)]\\
&\quad = F[D_0\,\Delta_{0;000} + D_1(\Delta_{0;100} + \Delta_{0;010} + \Delta_{0;001})\\
&\qquad + D_2(\Delta_{0;110} + \Delta_{0;101} + \Delta_{0;011}) + D_3\Delta_{0;111}]
\end{aligned} \tag{B6}$$

where the overall factor F, which will be absorbed in the normalization, does not concern us here and the coefficients D_j are given by (see Appendix A for the definition of t_λ)

$$\begin{aligned}
D_0 &= 1 - t_R^3 + 3t_R(t_R - 1)t_{2R}^2\\
D_1 &= -[(1 - t_R^3)t_{2R} + t_R(t_R - 1)t_{2R}^3 + 2t_R(t_R - 1)t_{2R}]\\
D_2 &= (1 - t_R^3)t_{2R}^2 + t_R(t_R - 1) + 2t_R(t_R - 1)t_{2R}^2\\
D_3 &= -[(1 - t_R^3)t_{2R}^3 + 3t_R(t_R - 1)t_{2R}]
\end{aligned} \tag{B7}$$

These ingredients allows us to construct the required expansion coefficients of the triangle probability

$$\begin{aligned}
c_{i;000} &= D_0 p_{i;000} + D_1(p_{i;100} + p_{i;010} + p_{i;001}) \\
&\quad + D_2(p_{i;110} + p_{i;101} + p_{i;011}) + D_3 p_{i;111} \\
c_{i;100} &= D_0 p_{i;100} + D_1(p_{i;000} + p_{i;110} + p_{i;101}) \\
&\quad + D_2(p_{i;010} + p_{i;001} + p_{i;111}) + D_3 p_{i;011} \\
c_{i;110} &= D_0 p_{i;110} + D_1(p_{i;010} + p_{i;100} + p_{i;111}) \\
&\quad + D_2(p_{i;000} + p_{i;011} + p_{i;101}) + D_3 p_{i;001} \\
c_{i;111} &= D_0 p_{i;111} + D_1(p_{i;011} + p_{i;101} + p_{i;110}) \\
&\quad + D_2(p_{i;001} + p_{i;010} + p_{i;100}) + D_3 p_{i;000}
\end{aligned} \tag{B8}$$

As before, the remaining coefficients can be obtained by suitably permuting the labels (jkl). Several quantities of interest can be immediately read off from these results; the magnetization of the spin in the center of the triangle is given by

$$m = \langle \sigma \rangle = \frac{c_{1;000}}{c_{0;000}} \tag{B9}$$

and the impurity concentration on any of the three vertices of the triangle is given by

$$n_1 = \frac{1}{2}(\langle \tau_1 \rangle + 1) = \frac{1}{2}\left(\frac{c_{0;100}}{c_{0;000}} + 1\right), \qquad \text{etc.} \tag{B10}$$

ACKNOWLEDGMENT

One of us (B.M.M.) was supported by a grant from the European Communities under contract 87400557/ST2*0444.

REFERENCES

1. V. J. Emery, *Phys. Rev. Lett.* **58**:2794 (1987).
2. A. Aharony, R. J. Birgenau, and M. A. Kastner, *IBM J. Res. Dev.* **33**:287 (1989).
3. K. de'Bell, *J. Phys. C: Solid State Phys.* **13**:L651 (1980).
4. Y. Kasai and I. Syozi, *Prog. Theor. Phys.* **50**:1182 (1973).
5. D. C. Mattis, *Phys. Rev. B* **38**:7061 (1988).
6. R. J. Vasconcelos dos Santos, I. P. Fittipaldi, P. Alstrom, and H. E. Stanley, *Phys. Rev. B* **40**:4527 (1989).

7. A. M. Szpilka, M. L. Glasser, D. C. Mattis, and M. P. Mattis, *Phase Transitions* **22**:185 (1990).
8. R. J. Elliot, *Phys. Rev.* **124**:698 (1961).
9. P. Bak and J. von Boehm, *Phys. Rev. B* **21**:5297 (1980).
10. J. Vannimenus, *Z. Phys. B: Condensed Matter* **43**:141 (1981).
11. S. Inawashiro, C. J. Thompson, and G. Honda, *J. Stat. Phys.* **33**:419 (1983).
12. M. J. de Oliviera, S. R. Salinas, and C. S. O. Yokoi, in *Fractals in Physics*, L. Pietronero, ed. (North-Holland, Amsterdam 1986).
13. T. Morita, *Physica* **83A**:411 (1976).
14. C. J. Thompson, *J. Stat. Phys.* **27**:441 (1982).
15. M. E. Issigoni and C. Papatriantafillou, *J. Stat. Phys.* **45**:527 (1986).
16. B. M. Mulder, Non-equivalence of ensembles in the ground state of a model with annealed impurities, *Physica* **174A** (1991).
17. G. Toulouse, *Comm. Phys.* **2**:115 (1977).
18. J. T. Chayes, L. Chayes, J. P. Sethna, and D. J. Thouless, *Commun. Math. Phys.* **106**:41 (1986).
19. C. Paraskevaidis and C. Papatriantafillou, Field induced particle pairing in an Ising system, *J. Stat. Phys.* **64**:385 (1991).